



University for the Common Good

Diagnosis of abnormal temperature rise observed on a 275 kv oil-filled cable surface: a case study

Yi, Huajie; Zhou, Chengke; Hepburn, Donald M.; Kearns, Martin; Peers, Graham

Published in:

IEEE Transactions on Dielectrics and Electrical Insulation

DOI:

[10.1109/TDEI.2018.007545](https://doi.org/10.1109/TDEI.2018.007545)

Publication date:

2019

Document Version

Peer reviewed version

[Link to publication in ResearchOnline](#)

Citation for published version (Harvard):

Yi, H, Zhou, C, Hepburn, DM, Kearns, M & Peers, G 2019, 'Diagnosis of abnormal temperature rise observed on a 275 kv oil-filled cable surface: a case study', *IEEE Transactions on Dielectrics and Electrical Insulation*, vol. 26, no. 2, pp. 547-553. <https://doi.org/10.1109/TDEI.2018.007545>

General rights

Copyright and moral rights for the publications made accessible in the public portal are retained by the authors and/or other copyright owners and it is a condition of accessing publications that users recognise and abide by the legal requirements associated with these rights.

Take down policy

If you believe that this document breaches copyright please view our takedown policy at <https://edshare.gcu.ac.uk/id/eprint/5179> for details of how to contact us.

Diagnosis of Abnormal Temperature Rise Observed on a 275 kV Oil-filled Cable Surface – A Case Study

Huajie Yi, Chengke Zhou and Donald M. Hepburn

Glasgow Caledonian University
School of Engineering and Built Environment
Glasgow, G4 0BA, UK

Martin Kearns and Graham Peers

EDF Energy
GSO Business Park, East Kilbride
Glasgow, G74 5PG, UK

ABSTRACT

This paper presents a case study on a 275 kV oil-filled cable. The condition assessment and diagnosis are based on analysis of cable surface temperature in relation to its current load and insulation dielectric loss. The work was initiated by a local abnormal temperature rise of 5.2 °C in cable surface temperature, which was observed during a routine inspection. The temperature rise occurred at bend area with a length of approximately one metre in the Blue Phase. No PD activity was identified using on-line PD measurement. The relation between cable surface temperature, cable core temperature and cable insulation condition was then simulated based on the thermal model of power cables. According to simulation analysis, poor condition of cable insulation or oil from an oil duct penetrating a region under the cable surface were identified as possible reasons for the problem observed. An in service X-ray scanning technique was employed for further investigation and to aid diagnosis. The X-ray images revealed a slight distortion of the PVC sheath and the presence of multiple voids between cable insulation paper and the lead sheath. It was concluded that an oil leakage from the oil duct to the voids under the cable lead sheath was responsible for the local cable surface temperature rise. The result removed the concern of incipient cable breakdown, and a potential unplanned outage.

Index Terms — oil filled cables, cable insulation, temperature measurement, liquid leak, X-ray imaging

1 INTRODUCTION

UNDER in-service conditions, the insulation in power cables is continuously subject to electrical, thermal, mechanical and environmental stresses. The reaction to inherent stresses may result in insulation degradation and, finally, failure [1]. Manufacturing defects, poor workmanship in installation and maintenance were identified as the major causes of cable failures [2,3]. Defects in cable insulation can lead to partial discharge (PD) activity, higher dielectric loss ($\tan \delta$) and heating [4-6].

A PD signal is a current pulse which has a duration of a few nanoseconds [7]. Cable PD activity is usually detected via high frequency current transformer (HFCT). PD can indicate any

local defect in cable insulation which has sufficient local electric field magnitude to initiate discharge [8]. Both on-line and off-line measurements of PD have been widely used in cable condition monitoring. Dielectric loss or dissipation factor is the value of the ratio of resistive current to capacitance current through cable insulation, as described in Figure 1. Dielectric losses consist of polarisation losses, conductivity losses and ionisation losses [9]. The movement of polarised molecules, ions and electrons, which are dependent on temperature and electrical field, determine the polarisation losses and conductivity losses [10]. $\tan \delta$, as indicated in equation (1), is inversely proportional to frequency. For operational reasons it is preferred that measurement of $\tan \delta$ is made under very low frequency excitation while the cable is switched out of circuit. Off-line insulation resistance (IR) measurement is usually based on the measurement of DC

leakage current [11]. The result varies as the change of

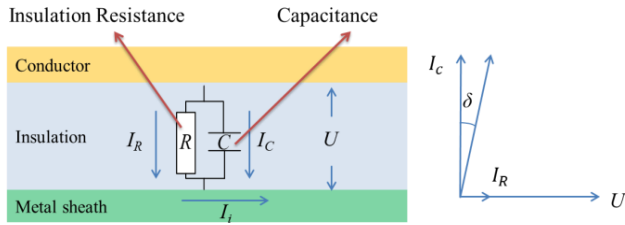


Figure 1. Dielectric loss.

insulation thickness and conductor surface area [12]:

$$\tan \delta = I_R / I_C = 1 / \omega RC. \quad (1)$$

A number of researchers have investigated cable condition monitoring via PD, $\tan \delta$ and cable insulation resistance (IR) measurement [11, 13, 14]. However, PD signals are sensitive to noise level [15] and the other two diagnosis methods cannot reflect local defect in cable insulation [14, 16]. This paper presents a case study which aims to explain the possible reasons for the local heating phenomenon in a one metre section of a 275 kV oil-filled (OF) cable.

Following the description of the problematic cable, the paper provides the results of PD tests which were carried out to detect local defects of the insulation. Then, through simulation of thermal effects of the cable in relation to current load and dielectric loss, two possible reasons behind the local temperature rise were derived. Finally, the study aims to confirm the explanations through the application of an in-service X-ray technique. The X-ray image on the cable indicates the presence of voids between paper insulation and lead sheath. It is believed that these were the cause of the local cable surface temperature rise.

2 CABLE CONSTRUCTION AND CASE DESCRIPTION

The cable was 275 kV OF with oil immersed sealing end established in a power station. The construction of the cable is shown in Figure 2 and cable details are provided in Table 1. The cable has been in operation for over 30 years. The full load that the cable is designed for is 128 A, but with the generator on nominal full load is actually only 26-28 A.

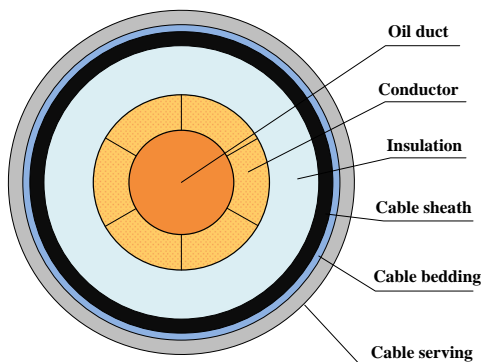


Figure 2. The configuration of the 275 kV OF cable.

As shown in Figure 3, the Blue phase is apparently bent between two cleats which are used to fix the cable. In Nov. 2017, an inspection via infrared thermal images of the three phase cable, at 6 °C ambient temperature, revealed a local cable surface temperature rise of 5.2 °C above other phases around the bent area of Blue phase (in Figure 4). In details, the temperature of Blue phase was 17 °C which was 11 °C rise above the ambient temperature, while the temperature of the other phases were 11.8 °C which were 5.8 °C higher than the ambient temperature.

Table 1. Dimension and Load Information for the 275 kV OF Cable.

Length	750m	Full load	128A
Conductor size	161.3mm ²	Inner diameter of insulation	19.7mm
External diameter	74.4mm	Outer diameter of insulation	59.1mm
Core	Copper	Sheath	Lead
Insulation	Paper	Serving	PVC



Figure 3. 275kV OF cable (Blue Phase) – the area marked in the green ellipse was observed to have a 5.2°C temperature rise.



Figure 4. Infrared thermal image of the Blue Phase.

The PD tests were carried out on the Jan 30th 2018. As shown in Figure 5, three HFCTs were clamped at the earthing strap of the cable terminations: these were connected to CH1, CH2 and CH3 of a bespoke DAQ box using BNC cables. The acquired data was then saved to laptop computer and analysed via specialist software. The test results are shown in Figure 6; examples of pulsative signals are highlighted in the ellipses in Figure 6a.

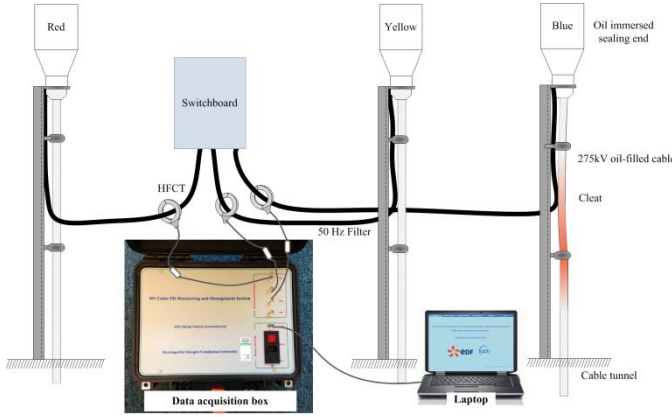
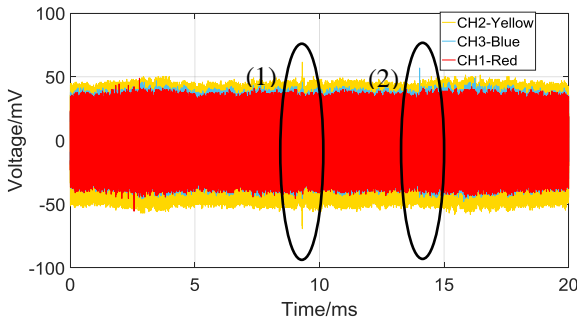
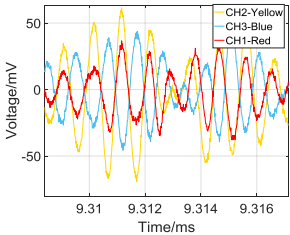


Figure 5. Physical connections of test instruments.

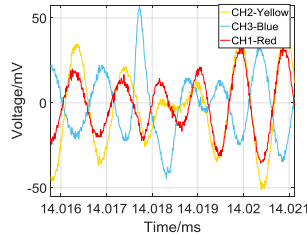
Oscillatory signals of high magnitude were observed from all three phases. Through analysis of pulse shape and signal phase resolved pattern, the signals are diagnosed as being noise. No PD pulse was detected in signals from the three phases. In detail, as shown in Figure 6b, the large pulse that is marked in Figure 6a as (1) has a frequency of around 1MHz with the RED phase showing the highest magnitude. As shown in Figure 6c, the frequency of the pulse indicated in Figure 6a as (2) has a frequency of 1.43MHz, with the Blue phase having the highest magnitude.



(a) Results of PD test, with all three-phase results overlaid



(b) Zoomed-in results at 9.315ms when CH2 has highest magnitude



(c) Zoomed-in results at 14.017ms when CH3 has highest magnitude

Figure 6. The results of PD test of the problem cable.

3 CALCULATION OF CABLE TEMPERATURE RISE

Since the traditional PD test could not explain the temperature rise in the OF cable, further investigation was required to determine the cause of the abnormal temperature rise in cable surface. Heating loss caused by insulation degradation is investigated in the following section.

3.1 THERMAL MODEL OF SING-CORE CABLE

According to IEC 60287 [17], the thermal model of a single-core cable can be mathematically assessed, as illustrated in Figure 7.

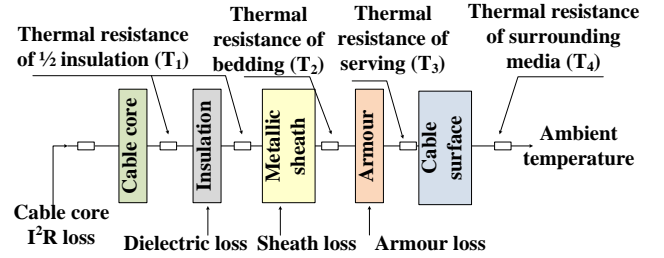


Figure 7. The schematic of thermal model of a power cable.

Two heating sources are responsible for cable temperature rise, i.e. cable conductors, including cable core and cable metallic sheath, and cable insulation. The load current and sheath current result in electrical losses and insulation deterioration leads to dielectric loss [18]. The equation to calculate the rise in temperature of the cable core in excess of ambient temperature is expressed as Equation (2):

$$\Delta\theta = \left(I^2 R + \frac{1}{2} W_d \right) T_1 + \left[I^2 R (1 + \lambda_1) + W_d \right] T_2 + \left[I^2 R (1 + \lambda_1 + \lambda_2) + W_d \right] (T_3 + T_4) \quad (2)$$

Here, R is the AC resistance per unit length of the cable core at actual operating temperature; I is the load current flowing in the cable core, (A); W_d is the dielectric loss per unit length of cable insulation, which is calculated from (3), (W/m); T_1 is the thermal resistance per unit length of cable insulation, (K.m/W); T_2 is the thermal resistance per unit length of the bedding between sheath and armour, (K.m/W); T_3 is the thermal resistance per unit length of the external serving of the cable, (K.m/W); T_4 is the thermal resistance per unit length of the surrounding media, (K.m/W); λ_1 is the ratio of losses in the metal sheath to total losses in all conductors in that cable; λ_2 is the ratio of losses in armouring to total losses in all conductors in that cable; $\Delta\theta$ is the cable core temperature rise above ambient temperature, ($^{\circ}\text{C}$),

$$W_d = U_0^2 \omega C \cdot \tan \delta \quad (3)$$

$$T_4 = \frac{1}{\pi D_e^* h (\Delta\theta_s)^{1/4}} \quad (4)$$

The dielectric losses of cable increase as the insulation deteriorates and thus $\Delta\theta$ becomes greater. T_4 , as expressed in Equation (4), is relevant to cable surface temperature, where $\Delta\theta_s$ is the cable surface temperature rise above ambient temperature, ($^{\circ}\text{C}$), and D_e^* is the external diameter of cable, (m). Equation (5) gives the relation between $\Delta\theta$

and $\Delta\theta_s$. By applying an iterative process, which is shown in Figure 8, both $\Delta\theta$ and $\Delta\theta_s$ can be determined.

$$(\Delta\theta_s)_{n+1}^{0.25} = \left[\frac{\Delta\theta + \Delta\theta_d}{1 + K_A (\Delta\theta_s)_n^{0.25}} \right]^{0.25} \quad (5)$$

where, $\Delta\theta_d$ is a factor to account for dielectric loss and K_A is a coefficient related to cable external diameter and thermal resistances T_1 , T_2 and T_3 .

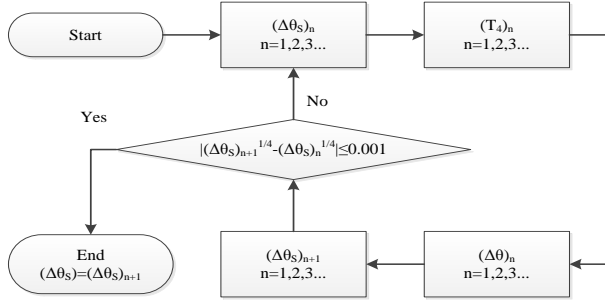


Figure 8. Flow chart of iterative process.

3.2 IMPROVED THERMAL MODEL FOR USE IN THE OF CABLE

The method for calculating cable temperature rise provided in IEC 60287 does not consider the effects of current in the metallic sheath for the only one single core cable. In the case study, the circulating current in each of the phases was found to be 5.6, 0.5 and 4.6A, respectively. As indicated in [19] and [20], unequal earthing resistance or the flat formation of the cables may be the reasons for the difference in sheath currents among the three phases. This is important as in this case, the sheath currents can be significant comparing with the load currents as cables are earthed at both ends. Since the separation distance among the three OF cables are great enough, the loss factor related to cable sheath loss (λ_1) and armour loss (λ_2), which are determined by the installation method of the three phase cables and cable construction, can be neglected. The revised cable thermal model for the case study is presented in Figure 9. The difference between cable core temperature and ambient temperature can be calculated from (6).

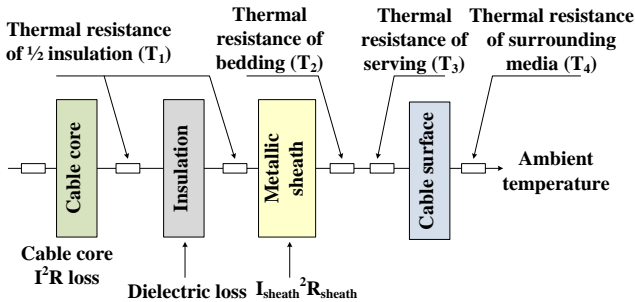


Figure 9. Schematic of the simplified thermal model for use in the case study.

$$\Delta\theta = \left(I^2 R + \frac{1}{2} W_d \right) T_1 + \left[I^2 R + I_{sheath}^2 R_{sheath} + W_d \right] T_2 + \left[I^2 R + I_{sheath}^2 R_{sheath} + W_d \right] (T_3 + T_4) \quad (6)$$

4 RESULTS AND POSSIBLE REASONS FOR CABLE SURFACE TEMPERATURE RISE

4.1 EFFECT OF SHEATH CURRENT ON TEMPERATURE RISE

As mentioned above, the circulating currents of three phases are unequal, perhaps due to variation in earthing resistance. Circulating currents flow in metallic sheaths and result in electric losses, which can reduce the current rating of the power cables [21]. The temperature rises in cable surface were calculated under different values of sheath currents, i.e. 0.5 and 5.6 A respectively.

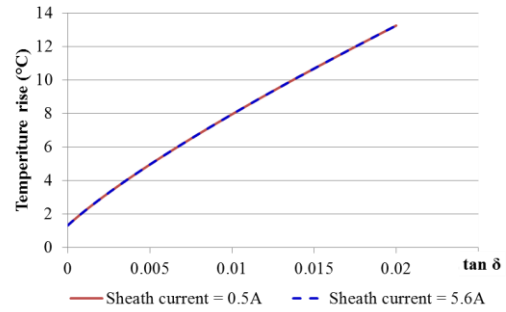


Figure 10. Cable surface temperature in excess of ambient temperature.

Figure 10 indicates that for the OF cable in the case study, the sheath currents has little effect on the cable surface temperature. Therefore the sheath current is not regarded as the reason for different temperature in the three phases.

4.2 REASON 1 - INSULATION DEGRADATION

The rise of cable core and cable surface temperature as the $\tan \delta$ increase is illustrated in Figure 11. It was reported that for oil-impregnated paper cable (see Table 2) in [22], when $\tan \delta$ is greater than 0.01, the cable insulation is assessed as being in bad condition and needing urgent action. Analysis shows that when $\tan \delta$ values are 0.0017 and 0.009, which correspond to good and considerably aged insulation conditions respectively, the corresponding cable surface temperatures are 5.8 and 11°C higher than ambient temperature correspondingly. In addition, if the $\tan \delta$ increases from 0.001 to 0.01, it causes a cable surface temperature rise of 5.97 °C.

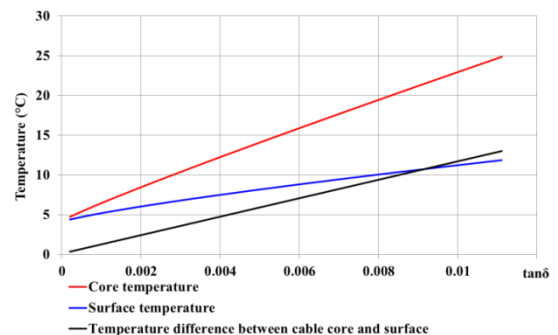


Figure 11. Temperature of cable core and cable surface for 26A load current at an ambient temperature of 6°C.

In the case study, because the cable section around the cleat is bent, it will have greater mechanical stress. The reason for a temperature rise in this region is more likely to be due to local insulation degradation rather than being due to moisture content, as quoted in the reference. It should be noted that the criterion for $\tan \delta$ given in Table 2 is measured at an ambient temperature of 20°C. However, the ambient temperature was only 6 °C when the problem was observed and the $\tan \delta$ of oil insulation is more temperature sensitive than that for extruded insulations [23]. According to the results from [24], in the temperature range from 6 to 20 °C, the value of $\tan \delta$ decreases as the cable core and surface temperature rises. Therefore, the $\tan \delta$ value of the cable insulation should be greater at an ambient temperature of 6 °C. Consequently it can be concluded that a local surface temperature rise of 5.2 °C could be the result of locally aged insulation, and the degradation is under the threshold of moderately aged by the standards provided in [22].

Table 2. Criteria for $\tan \delta$ of Oil-impregnated paper cable [22].

Minimum $\tan \delta$	Estimated average moisture [%]	Condition
0.002-0.0035	Below 1	Good
0.0035-0.0050	1-2.5	Moderately aged
0.0050-0.010	2.5-3.5	Considerably aged
Above 0.010	Above 3.5	Bad condition

4.3 REASON 2: LEAKAGE OF WARM OIL FROM OIL DUCT TO UNDER THE CABLE SURFACE

For the Self-Contained OF cable used in the case study, the oil from the oil duct is allowed to flow through the cable core and it fills the free spaces between the core and insulation paper [25]. Since the oil duct is surrounded by the cable core, it is probable that the temperature of oil is as high as that of the cable core for long operating periods.

Figure 11 also suggested that as $\tan \delta$ increase, the temperature difference between cable core and cable surface becomes greater. When $\tan \delta$ is 0.0031, for which cable insulation can be assessed as in good condition, cable core temperature is 6 °C above ambient temperature. Therefore another reason which explains the thermal problem observed would be an oil leakage from the cable core to under the cable surface without the cable insulation severely deteriorating. As a result, oil with higher temperature leaking from the oil duct through an existing path would infuse higher temperature oil through the insulated paper and result in a cable surface temperature rise.

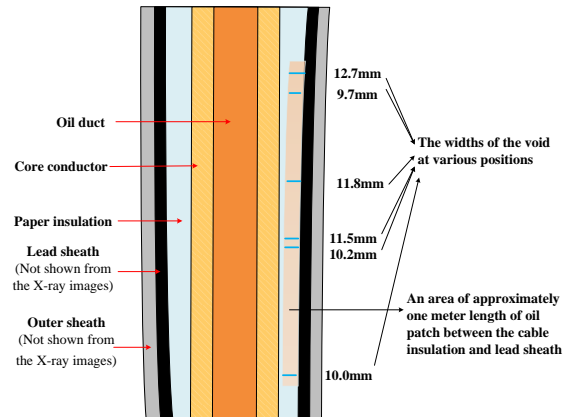
5 DIAGNOSIS BASED ON X-RAY TECHNIQUE

An X-ray technique was used to help researchers confirm the proposed fault diagnoses. The X-ray images were taken from both front and back side of the Blue Phase, as shown in Figure 12a and Figure 12b, respectively. Cable

construction is clearly displayed in the two X-ray images. Slight distortion of the cable can be demonstrated from inconsistent outer diameters of lead sheath, which are 66.2 and 66.0 mm respectively, and various thickness of the lead sheath which are 2.9, 3.2 and 3.0 mm respectively. The red ellipses in Figure 12a and Figure 12b show the oil region between the cable insulation and lead sheath, this has different widths at various positions.



(a) Front images (b) Rear images
– the red ellipse shows the area of oil leakage



(c) Schematic diagram of the X-ray results, a representation of the front and rear X-ray images

Figure 12. X-ray images of Blue Phase cable acquired on March 22nd 2018.

The images show that the thickness of the lead sheath varies, i.e. 3.2, 3.0 and 2.9 mm. The diameter of the conductor is shown to be 18.1 mm and the outer diameter of the lead sheath is shown to vary between 66.2 and 66.0 mm. The X-ray images also indicate a narrow region between cable insulation and lead sheath filled with oil. The lengths of the void at various positions in Figure 12a are measured as 9.7, 10.0 and 10.2 mm and in Figure 12b as 12.7, 11.8 and 11.5 mm. As shown in Figure 12c, an oil filled region between the cable insulation and lead sheath, approximately one meter in length, may have been responsible for the abnormal temperature rise. As shown in Figure 13, channels formed due to distortion and deformation allow the higher

temperature oil in the duct to move to under the cable surface, resulting in a local cable surface temperature rise.

The above analysis confirms that oil leakage through the voids between cable insulation and lead sheath is the most likely explanation for the temperature increase.

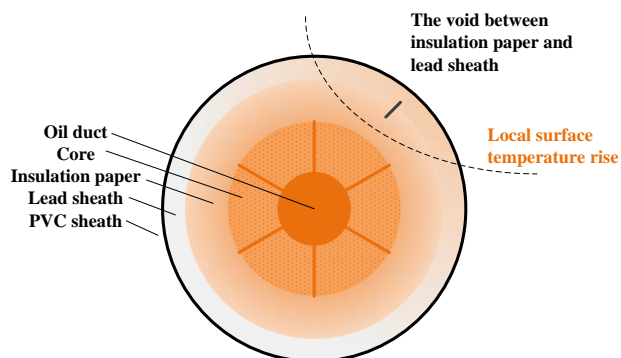


Figure 13. Cross section of OF cable showing area filled with hot insulation oil.

6 CONCLUSIONS

The case study has presented the diagnosis result of an abnormal local temperature rise in the surface of an OF cable. No cable PD activity was found during an online monitoring campaign. Cable surface and core temperature were then simulated based on the improved thermal model to analyse the insulation condition. Results revealed that degradation of cable insulation causes both cable surface and cable core temperatures to increase, meaning that the local temperature rise could be due to either leakage of warm oil from the oil duct in the centre of the cable to below the cable surface, or local insulation degradation. The X-ray images indicated that the oil-leakage was the reason for the problem as observed. In total five voids and channels were found between the cable insulation and lead sheath, and thus the oil from oil duct which had higher temperature would impregnate the insulation paper and caused local temperature rise.

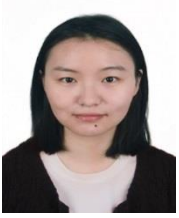
The result removed the concern of incipient cable breakdown, and a potential unplanned outage, which could cost multimillion pounds per day.

ACKNOWLEDGMENT

The authors would like to thank EDF Energy for their support and financial assistance for the research work.

REFERENCES

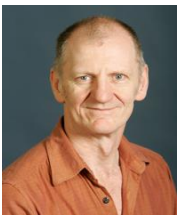
- [1] J. Densley, "Ageing mechanisms and diagnostics for power cables - an overview," *IEEE Electr. Insul. Mag.*, vol. 17, no. 1, pp. 14-22, Jan.-Feb. 2001.
- [2] B. Van Maanen, C. Plet, P. Van Der Wielen, et al., "Failures in underground power cables – return of experience," *IEEE Int. Conf. Insulated Power Cables*, 2015, pp. 1-5.
- [3] Z. Tang et al., "Analysis of Significant Factors on Cable Failure Using the Cox Proportional Hazard Model," *IEEE Trans. Power Del.*, vol. 29, no. 2, pp. 951-957, April 2014.
- [4] IEEE Guide for Partial Discharge Testing of Shielded Power Cable Systems in a Field Environment, IEEE Std 400.3-2006, 2007-02-05.
- [5] J. Densley, "An overview of aging mechanisms and diagnostics for extruded power cables," *IEEE Power Engineering Society Winter Meeting Conf.*, 2000, vol. 3, pp. 1587-1592.
- [6] A.N. Lubkov, I.N. Privalov, V.A. Mezgin, "Diagnostics of the insulation of high-pressure oil-filled 220- and 500-kV cable lines when operating in hydroelectric power plant," *Power Technology and Engineering*, vol. 45, no 1, pp 69 - 75, May 2011.
- [7] S. A. Boggs, "Partial discharge. II. Detection sensitivity," *IEEE Electr. Insul. Mag.*, vol. 6, no. 5, pp. 35-42, 1990.
- [8] F. Yang, X. Feng, L. Ruan and J. Chen, "Research on the diagnosis of MV power cable insulation based on PD and VLF-Tan δ ," *IEEE Int. Conf. Electr. Electron. Sys. Eng. (ICEESE)*, 2014, pp. 123-127.
- [9] C. Freitag, I. Mladenovic and C. Weindl, "Experiences of in field measured dissipation factor on MV PILC cables at 50 Hz," *22nd Int. Conf. Exhibition on Electricity Distribution (CIRED)*, 2013, pp. 1-4.
- [10] I. Mladenovic and C. Weindl, "Dependencies of the PD- and tan (δ)-characteristics on the temperature and ageing status of MV PILC cables," *Annu. Rep. Conf. Electr. Insul. Dielectr. Phenom.(CEIDP)*, 2011, pp. 88-92.
- [11] D. L. McKinnon, "Insulation Resistance Profile (IRP) and its use for assessing insulation systems," *IEEE Int. Sympos. Electr. Insul (ISEI)*, 2010, pp. 1-4.
- [12] IEEE Recommended Practice for Testing Insulation Resistance in Electric Machinery, IEEE Std 43-2013 (Revision of IEEE Std 43-2000).
- [13] A. Nakajima et al., "Development of a hot-line diagnostic method for XLPE cables and the measurement results", *IEEE Trans. Power Del.*, vol. 4, no. 2, pp. 857-862, Apr 1989.
- [14] S. I. Yamaguchi, S. Soda and N. Takada, "Development of a new type insulation diagnostic method for hot-line XLPE cables," *IEEE Trans. on Power Del.*, vol. 4, no. 3, pp. 1513-1520, Jul 1989.
- [15] G. C. Stone, "Partial discharge. VII. Practical techniques for measuring PD in operating equipment," *IEEE Electr. Insul. Mag.*, vol. 7, no. 4, pp. 9-19, July-Aug. 1991.
- [16] H. Sun, L. Lu, J. Lu, et al, "Research on a mixed method of the on-line monitoring of high voltage power cable with XLPE insulation," *Int. Conf. Electr. Machines and Systems*, 2003, vol.2, pp. 844-847.
- [17] Electric cables - Calculation of the current rating - Part1-1: Current rating equations (100 % load factor) and calculation of losses – General, IEC 60287-1-1:2006+A1:2014, 2014-11-30.
- [18] Y. Liang, Q. Liu, H. Sun and Y. Li, "Cable load dynamic adjustment based on surface temperature and thermal circuit model," *IEEE Int. Conf. on Condition Monitoring and Diagnosis (ICCMD)*, 2008, pp. 705-708.
- [19] A.M. Amin Hussein, "Effect of the Fault Impedance on the Performance of Directional Over Current Relays in Medium Voltage Power Cables- A Case Study," *IEEE Int. Conf. Insulated Power Cables*, 2015, pp. 1-6.
- [20] M. Marzinotto and G. Mazzanti, "The Feasibility of Cable Sheath Fault Detection by Monitoring Sheath-to-Ground Currents at the Ends of Cross-Bonding Sections," in *IEEE Trans. Ind. Appl.*, vol. 51, no. 6, pp. 5376-5384, 2015.
- [21] Standard for the Testing, Design, Installation, and Maintenance of Electrical Resistance Trace Heating for Industrial Applications, IEEE Std 515-2011 (Revision of IEEE Std 515-2004) - Redline, 2011-09-09.
- [22] S. Banerjee, A. Naderian and H. Sedding, "Off-Line Field Diagnostics for MV and HV Oil-Paper Insulated Cables," *24th Nordic Insulation Symposium on Materials, Components and Diagnostics*, 2015, pp. 15 -17.
- [23] Guide for Field Testing and Evaluation of the Insulation of Shielded Power Cable Systems Rated 5 kV and Above, IEEE Std 400-2012 (Revision of IEEE Std 400-2001) , 2012-06-05.
- [24] S. Kagaya, T. Yamamoto and A. Inohana, "Aging of Oil-Filled Cable Dielectrics," *IEEE Trans. on Power App. Sys.*, vol. PAS-89, no. 7, pp. 1420-1428, Sept. 1970.
- [25] C.R. Bayliss and B.J. Hardy, "Cables, In Transmission and Distribution Electrical Engineering (Fourth Edition)," Newnes, Oxford, Pages 397-466, 2012.



Huajie Yi (S'17), a PhD student at Glasgow Caledonian University (GCU), Glasgow, U.K., was born in Hubei Province, China, 1993. She received her B.Sc. degree in Electrical Engineering and Automation and M.Sc. degree in Electrical Engineering from Wuhan University, Wuhan, China, in 2014 and 2016, respectively. Her research interests include cable condition assessment through PD monitoring, dielectric loss and leakage current measurement under in service condition.



Chengke Zhou (M'06-SM'13) received his B.Sc. and M.Sc. degrees in Electrical Engineering from Huazhong University of Science and Technology, Wuhan, China, in 1983 and 1986, respectively, and the Ph.D. degree in Electrical Engineering from The University of Manchester, Manchester, U.K., in 1994. He is a currently Professor in the School of Computing, Engineering and Built Environment, Glasgow Caledonian University (GCU), Glasgow, U.K. Prof Zhou has over 30 years research experience in power systems and HV condition monitoring and has published over 40 papers in IET Journal and IEEE Transactions, among the 180 papers he has published in the area. Prof. Zhou is a Chartered Engineer, Fellow of IET and SMIEEE.



Donald M. Hepburn (M'08) received his B.A. (Hons) from the Open University in 1987 and Ph.D. degree from Glasgow Caledonian University (GCU) in 1994. He is a Senior Lecturer at GCU, a member of the IEEE, Institute of Physics, the IET and C.Eng. He has 20 years of industrial research experience and has been involved in research into HV insulation systems at GCU for over 20 years. His research interests cover monitoring physical and chemical change in HV/MV insulation materials and application of advanced digital signal processing to information from electrical, acoustic and RF monitoring techniques.



Martin Kearns received a B.Eng. degree in Electrical and Electronic Engineering from Strathclyde University, UK in 1990. Since then, he has worked in the UK nuclear industry and is currently the Chief Electrical Engineer in EDF Energy, Nuclear Generation. He is a Chartered Engineer and Fellow of the IET.